Metabolic Activation of Pyrrolizidine Alkaloids: Insights into the Structural and Enzymatic Basis

ARTICLE *in* CHEMICAL RESEARCH IN TOXICOLOGY · MAY 2014

Impact Factor: 3.53 · DOI: 10.1021/tx500071q · Source: PubMed

5 AUTHORS, INCLUDING:

Yang Ye
Chinese Academy of Sciences
139 PUBLICATIONS **2,023** CITATIONS
SEE PROFILE

Ge Lin
The Chinese University of Hong Kong
178 PUBLICATIONS **3,322** CITATIONS
SEE PROFILE

Chemical Research in Toxicology

Article

pubs.acs.org/crt

Metabolic Activation of Pyrrolizidine Alkaloids: Insights into the Structural and Enzymatic Basis

Jianqing Ruan,[†,‡] Mengbi Yang,[†,‡] Peter Fu,[§] Yang Ye,[‡,∥] and Ge Lin*[,†,‡]

[†]School of Biomedical Sciences, The Chinese University of Hong Kong, Hong Kong SAR, P.R. China

[‡]Joint Research Laboratory for Promoting Globalization of Traditional Chinese Medicines between Shanghai Institute of Materia Medica, Chinese Academy of Sciences, and The Chinese University of Hong Kong, Hong Kong SAR, P.R. China

[§]National Center for Toxicological Research, U.S. Food and Drug Administration, 3900 NCTR Road, Jefferson, Arkansas 72079, United States

[∥]State Key Laboratory of Drug Research & Natural Products Chemistry Department, Shanghai Institute of Materia Medica, Chinese Academy of Sciences, 555 Zu Chong Zhi Road, Zhang Jiang Hi-Tech Park, Pudong, Shanghai 201203, P.R. China

ABSTRACT: Pyrrolizidine alkaloids (PAs) are natural toxins widely distributed in plants. The toxic potencies of different PAs vary significantly. PAs are mono- or diesters of necine acids with a necine base. On the basis of the necine bases, PAs are classified into three types: retronecine-type, otonecine-type, and platynecine-type. Hepatotoxic PAs contain an unsaturated necine base. PAs exert hepatotoxicity through metabolic activation by hepatic cytochromes P450s (CYPs) to generate reactive intermediates which form pyrrole−protein adducts. These adducts provide a mechanism-based biomarker to assess PA toxicity. In the present study, metabolic activation of 12 PAs from three structural types was investigated first in mice to demonstrate significant variations in hepatic metabolic activation of different PAs. Subsequently, the structural and enzymatic factors affecting metabolic activation of these PAs were further investigated by using human liver microsomes and recombinant human CYPs. Pyrrole−protein adducts were detected in the liver and blood of mice and the *in vitro* systems treated with toxic retronecine-type and otonecine-type PAs having unsaturated necine bases but not with a platynecine-type PA containing a saturated necine base. Retronecine-type PAs produced more pyrrole−protein adducts than otonecine-type PAs with similar necine acids, demonstrating that the structure of necine base affected PA toxic potency. Among retronecine-type PAs, open-ring diesters generated the highest amount of pyrrole−protein adducts, followed by macrocyclic diesters, while monoesters produced the least. Only CYP3A4 and CYP3A5 activated otonecine-type PAs, while all 10 CYPs studied showed the ability to activate retronecine-type PAs. Moreover, the contribution of major CYPs involved also varied significantly among retronecine-type PAs. In conclusion, our findings provide a scientific basis for predicting the toxicities of individual PAs in biological systems based on PA structural features and on the pattern of expression and the selectivity of the CYP isoforms present.

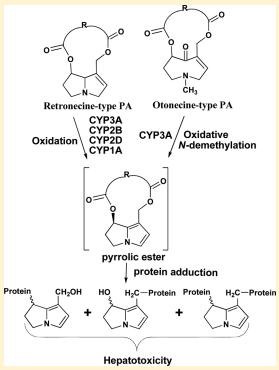

INTRODUCTION

Pyrrolizidine alkaloids (PAs) occur naturally in about 3% of the world's flowering plants.[1] To date, more than 660 PAs and PA *N*-oxides have been identified in over 6000 plants,and about half of them have been reported to be toxic to various organs, especially the liver.[2] Numerous plants used for herbal medicines are known to contain toxic PAs,and the contamination of foods and food supplements with PAs is also likely. Consequently, human PA poisonings from the intake of herbs or foodstuffs containing PA have been reported worldwide.[2−5] Additional cases of PA-induced hepatotoxicity may not be documented due to the lack of a well-established worldwide record system and the unavailability of specific and confirmative diagnoses.

PAs consist of a necine base and one or two necic acids. Toxic PAs are mono- or diesters of C1−C2 unsaturated necine base. PAs are classified into three general types based on the structure of their necine bases (Figure 1A): retronecine-type, otonecine-type, and platynecine-type (Figure 1B). The most toxic PAs are those belonging to the retronecine-type, which include mono- or diesters at C7 and C9 positions. Retronecine-type and otonecine-type PAs, which have a C1−C2 double bond in their unsaturated necine base, are hepatotoxic, while platynecine-type PAs that have a saturated necine base are non/less-toxic.[2,3,6,7] PAs are pro-toxins and require hepatic metabolic activation to generate reactive metabolites to exert toxicity. The metabolic activation of retronecine-type PAs involves an oxidation pathway to form pyrrolic esters (Figure 2), which are highly reactive and nonspecifically bind with cellular protein to form pyrrole−protein adducts leading to acute toxicity mainly in the liver and also other organs, such as the lung.[3,8] Pyrrolic esters also react with DNA to form pyrrole−DNA adducts exhibiting genotoxicity.[2,3,9] The reactive pyrrolic esters having two functional groups at C7 and C9 positions have also been demonstrated *in vitro* to form the adducts of pyrrole−protein−protein, pyrrole−DNA−DNA, and pyrrole−DNA−protein cross-links, leading to toxicity in different organs, in particular the liver.[9−14] On a structure−

Received: March 3, 2014
Published: May 16, 2014

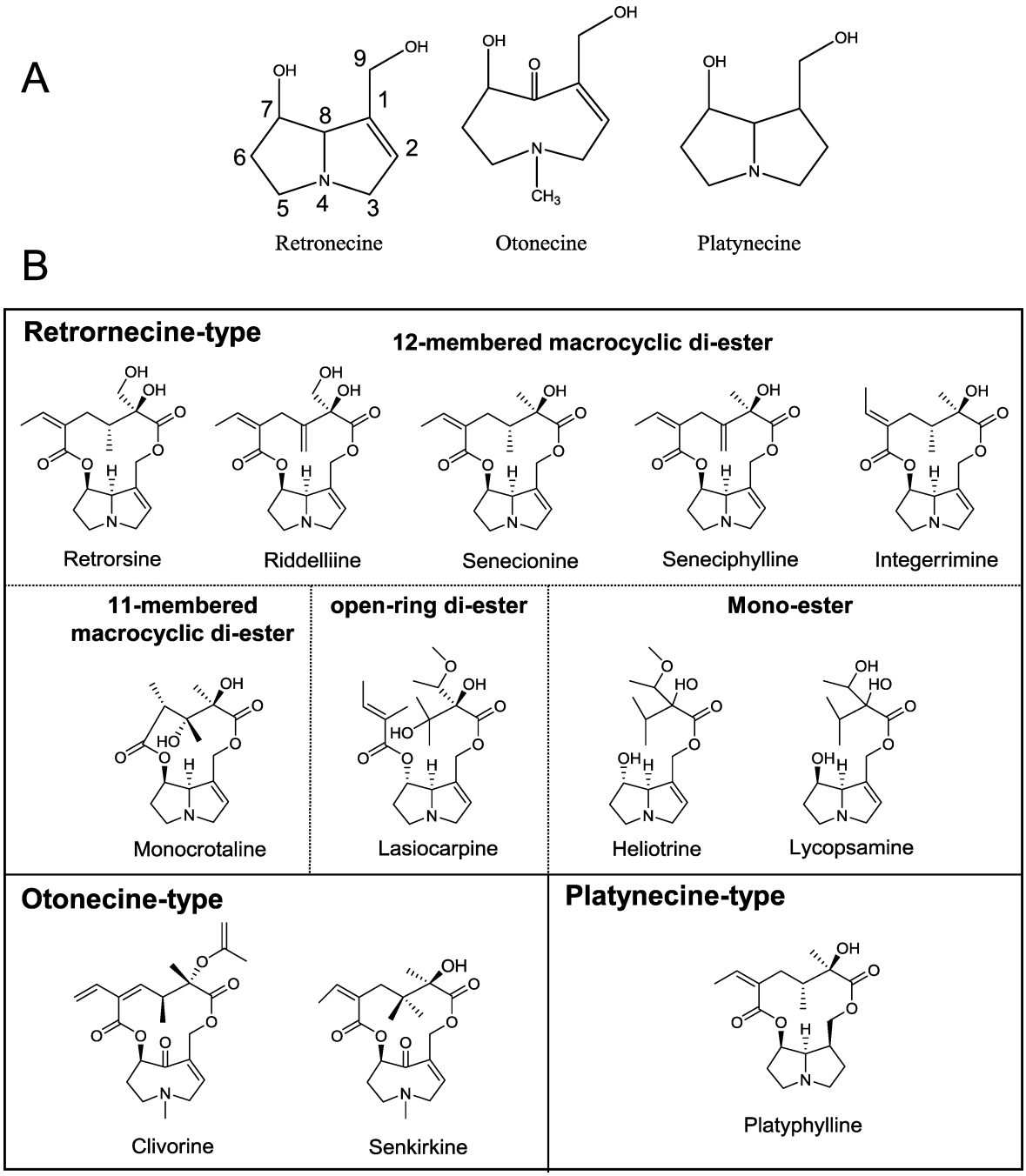

Figure 1. Chemical structures of the necine bases (A) and 12 PAs studied (B). Different PAs were divided into three types according to their necine base: retrornecine-type, otonecine-type, and platynecine-type. Retrornecine-type PAs were further divided into four subgroups: 12-membered macrocyclic diester, 11-membered macrocyclic diester, open-ring diester, and monoester.

activity relationship basis, Coulombe and co-workers studied the induction of pyrrole−DNA−DNA and pyrrole−DNA−protein cross-linking of several PAs in cultured bovine kidney epithelial cells with an external metabolizing system.[10,12,14] The results indicated that PAs with different structural features exhibited different pyrrole−DNA−DNA and pyrrole−DNA−protein cross-linking activities and also produced markedly different cytotoxic potencies, implying that such cross-linking activity was involved in PA-related toxicity. The metabolic activation of otonecine-type PAs is similar but with an initial oxidative *N*-demethylation step (Figure 2).[15] Pyrrolic esters also bind with glutathione (GSH) to form GSH conjugates, which are readily excreted as an important detoxification pathway.[16,17] Many studies reported that hepatic cytochromes P450 (CYP), especially CYP3A and CYP2B subfamilies, catalyze the metabolic activation of both toxic types of PAs in rodents,[3,17,18] while only limited data indicate that human CYP3A4 mediates PA metabolic activation.[19]

Pyrrolic esters are believed to be an important and primary cause responsible for the hepatoxicity of PAs.[3,6] However, such reactive metabolites could not be directly determined due to their instability, while pyrrole−protein adducts are relatively stable in the body. Recently, we developed a specific and sensitive LC-MS method for analyzing pyrrole−protein adducts

dx.doi.org/10.1021/tx500071q | *Chem. Res. Toxicol.* 2014, 27, 1030−1039

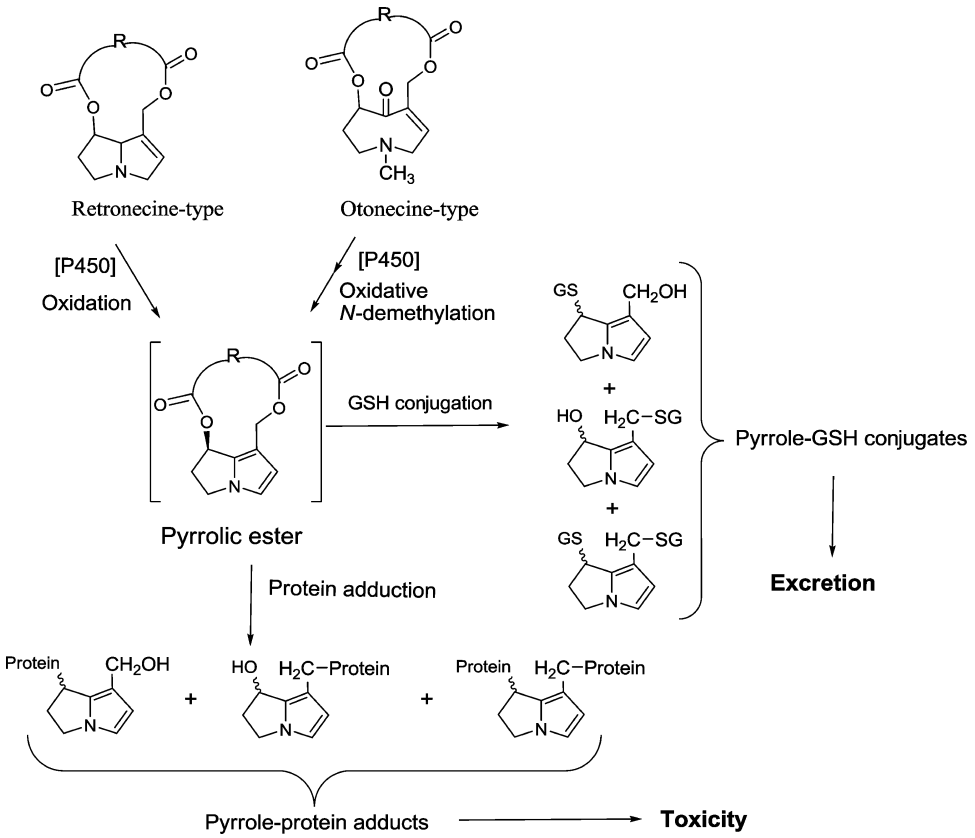

Figure 2. Proposed hepatic metabolic activation of retronecine-type and otonecine-type PAs to form pyrrolic esters, which further interact with glutathione or proteins to generate pyrrole−GSH conjugates or pyrrole−protein adducts, respectively.

and successfully determined blood pyrrole−protein adducts in patients who ingested PA-containing herbs and in rats treated with herbal extracts containing PA.[20,21] Therefore, in addition to pyrrole−DNA−protein cross-linking formation being considered as a potential biomarker of PA-induced toxicity,[10−14] we anticipated that pyrrole−protein adducts represent the metabolic activation fate of PAs and thus can serve as a specific mechanism-based biomarker.

Because of a high risk of PA exposure and its significant impact in public health, regulations have been enacted to restrict the use of PA-containing products.[22,23] However, these regulations differed significantly and were established based on the estimated amounts of PAs ingested in individual PA poisoning cases, especially acute liver injuries. For instance, the lowest limits of PA exposure at 1.0 μg/day for ≤6 weeks and 0.1 μg/day for ≥6 weeks were set by German Federal Health Bureau,[24] while a high dose limit of 15 μg/kg/day was suggested by World Health Organization.[25] It is well known that hepatotoxic potency varies markedly among different PAs.[26] On the basis of the mechanism of hepatotoxicity, the severity of PA toxicity depends on various factors, including metabolic activation rates, pyrrole−protein adduct formation, and GSH detoxification to convert reactive pyrrolic esters into pyrrole−GSH conjugates, which are readily excreted. However, important information about these critical factors affecting PA poisonings in humans is lacking.

An improved understanding of the PA structure−toxicity relationship will provide a better rationale for predicting the toxicity of different PAs, and this insight will benefit risk assessment efforts involved in establishing appropriate regulatory limits for PA exposure. Therefore, a systematic investigation of the structure−toxicity relationship for different PA types is necessary. In the present study, particularly focusing on the acute hepatotoxicity induced by hepatic metabolic activation of toxic PAs, we used the formation of pyrrole−protein adducts in mice as a biomarker to first demonstrate significant variations in the *in vivo* metabolic activation efficiency of 12 PAs that represent the three PA structural types. Afterward, the in-depth evaluation of the structure−toxicity relationship of these PAs was further performed in human liver microsomal incubations. The results revealed a structural basis affecting the efficiency of PA metabolic activation. Moreover, the *in vitro* incubations of different PAs with recombinant human CYPs were also evaluated to provide additional mechanistic insights regarding how PA structural features influenced the substrate selectivity by different CYP isoforms mediating the metabolic activation of different types of PAs.

MATERIALS AND METHODS

Chemicals. Twelve PAs were used in the study. Eight PAs, including monocrotaline and retrorsine (Sigma Chemical Co., St. Louis, MO), seneciphylline, senecionine, and senkirkine (ChromaDex Co., Irvine, CA), heliotrine (Accurate Chemical & Scientific Co., Westbury, NY), and lycopsamine and lasiocarpine (Phytolab, Vestenbergsgreuth, Germany), were purchased commercially. For the other four PAs, clivorine was isolated from *Ligularia hodgsonii* Hook. Integerrimine and platyphylline (mixed with 30% neoplatyphylline) were kindly provided by Professor Hai Shen Chen from Department of Phytochemistry, The Secondary Military Medical University, China. Riddelliine was provided by Dr. Po-Cheun Chan of the U.S. National Toxicology Program. The purity and identity of these four PAs were examined and confirmed in our laboratory as

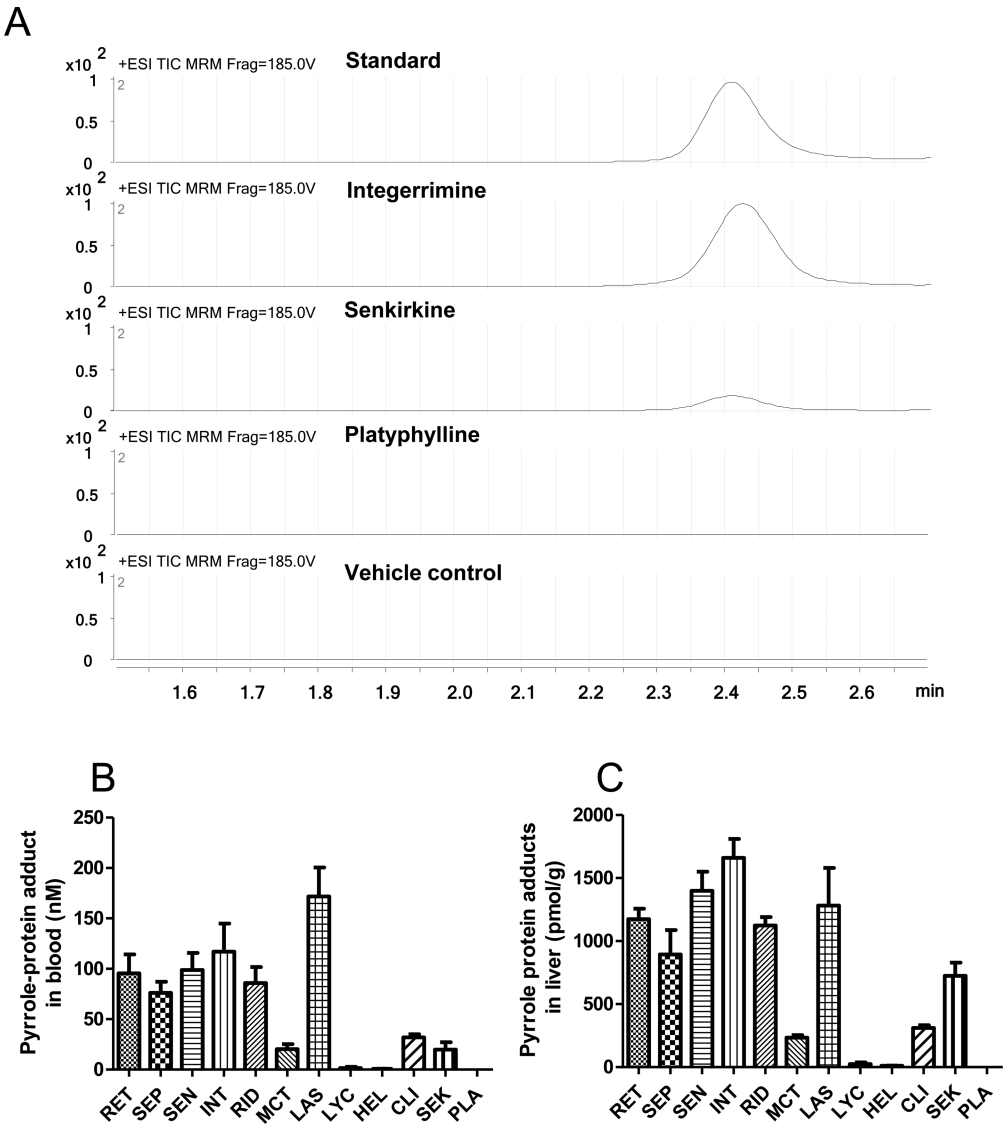

Figure 3. Representative MRM chromatograms of the standard (pyrrole−GSH conjugate, 7,9-diGSH-DHP) and blood samples obtained from the mice treated with vehicle, integerrimine, senkirkine, and platyphylline, representing retronecine-type, otonecine-type, and platynecine-type of PAs, respectively (A). Pyrrole−protein adduct levels in the blood (B) and liver (C) samples obtained from the mice treated with different PAs. Abbreviations used for individual PAs: retrorsine, RET; seneciphylline, SEP; senecionine, SEN; integerrimine, INT; riddelliine, RID; monocrotaline, MCT; lasiocarpine, LAS; lycopsamine, LYC; heliotrine, HEL; clivorine, CLI; senkirkine, SEK; and platyphylline, PLA.

reported previously.[27−29] Two pyrrole−GSH conjugates, namely, 7-GSH-DHP and 7,9-diGSH-DHP (having monoglutathionyl substitution at the 7(±) position in DHP (6,7-dihydro-7-hydroxy-1-hydroxymethyl-5*H*-pyrrolizine) and diglutathionyl substitutions at 7,9-(±) positions in DHP, respectively) (Figure 2), were isolated from scaled-up rat liver microsomal incubations as reported previously[15] and used as standards for HPLC-UV analyses. Human liver microsomes and human recombinant CYP Supersomes were purchased from BD Gentest (Woburn, MA). HPLC-grade acetonitrile and methanol (E. Merck, Darmstadt, Germany) were used for HPLC analyses, and all other chemicals were purchased from Sigma Chemical Co. (St. Louis, MO).

Treatment of Mice with PAs. The use of animals was approved by the Animal Experimental Ethics Committee, The Chinese University of Hong Kong. Male ICR mice (20−25 g) were supplied by the Laboratory Animal Services Centre at The Chinese University of Hong Kong. Mice in different groups (n = 3) were treated with individual PAs at a single dose of 20 μmol/kg intraperitoneally for 24 h. For the dosage regimen, the dose used was based on the retrorsine dose that induced liver injury in laboratory animal models in our previous study of different dosages of retrorsine (unpublished data in Ruan, J. Q. (2013), Ph.D. Thesis, The Chinese University of Hong Kong), while the treatment time was chosen based on our previous study in which among various treatment periods, the alteration of general biomarkers for liver injury, such as the elevation of serum ALT level, was more significant after a 24 h treatment of retrorsine.[30] After treatment, blood and liver samples were collected, serum was freshly prepared from each blood sample collected, and all specimens were stored at −80 °C until analysis.

***In Vitro* Hepatic Metabolism of PAs.** The procedure for incubations of PA samples with hepatic microsomes described previously was adopted for the present study.[7,31] Briefly, individual PAs (200 μM) were incubated in reaction mixtures with 100 mM potassium phosphate buffer (0.2 mL, pH 7.4) containing an NADPH-regenerating system (5 mM $MgCl_2$, 1 mM NADP+, 1 mM glucose 6-phosphate and 1 U/mL glucose-6-phosphate dehydrogenase) and different human CYP Supersomes (100 pmol/mL) or human liver microsomes (1 mg/mL) in the presence of 2 mM GSH. Excess GSH was included to trap the reactive pyrrolic esters generated by toxic PAs to form pyrrole−GSH conjugates. After incubation for 2 h, the

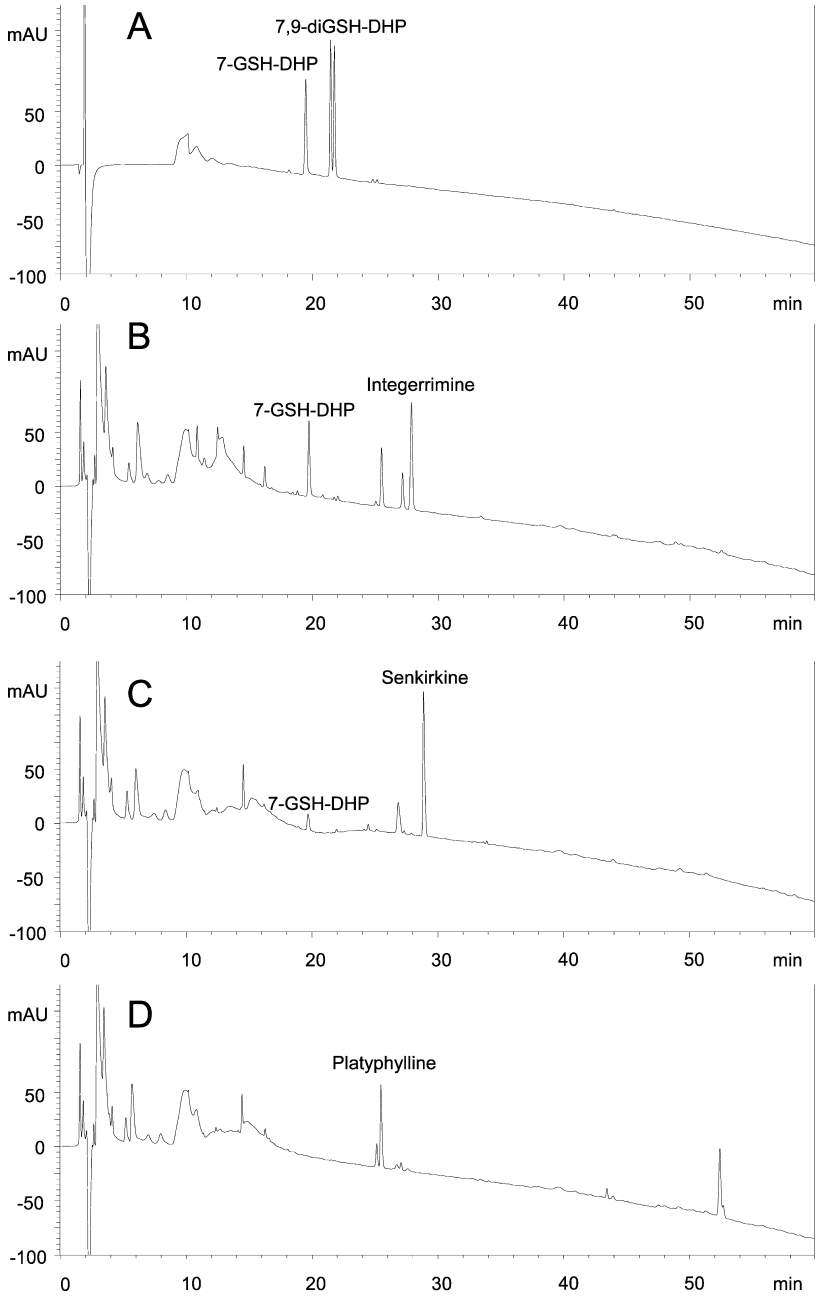

Figure 4. Representative HPLC-UV chromatograms of 7-GSH-DHP and 7,9-diGSH-DHP standards (A), and incubates of human liver microsomes in the presence of GSH with integerrimine (B), senkirkine (C), and platyphylline (D), representing retronecine-type, otonecine-type, and platynecine-type PAs, respectively.

reactions were stopped by chilling in ice water, and the resultant incubates were centrifuged at 4 °C at 15,000*g* for 20 min. The supernatants were collected and filtered through 0.45 μm membrane filters for HPLC-UV analysis of unreacted PA and pyrrole−GSH adduct levels. The residual protein pellets were collected for the measurement of pyrrole−protein adducts.

Determination of Pyrrole−Protein Adducts. Individual serum (100 μL) and liver (100 μg) samples collected from treated mice and the residual protein pellets obtained from metabolic incubation were derivatized using our previously developed method.[20] Briefly, each sample was mixed with 500 μL of acetone, vortexed, and centrifuged at 900*g* for 5 min. After washing with absolute ethanol, the pellets were reconstituted into 100 μL of 2% silver nitrate ethanol solution and shaken for 30 min at room temperature followed by reacting with 4-dimethylaminobenzaldehyde (v/v 4:1) in ethanol containing 1% perchloric acid at 55 °C for 10 min. The resultant mixtures were filtered and then subjected to UHPLC-MS analysis. For the quantitation of pyrrole−protein adducts, 7,9-diGSH-DHP was also derivatized under the same condition and used as a standard to construct the calibration curve used for the determination of the pyrrole-derived analyte formed via derivatization of the DHP moiety released from pyrrole−protein adducts.[20] It is noted that the quantified total amount of the adducts might contain a combination of pyrrole−protein adducts and pyrrole−protein−protein cross-links (Figure 2) in both *in vitro* and *in vivo* samples. In addition, pyrrole-DNA−protein cross-links[9−14] might also be formed in the biological specimens of PA-treated mice, especially in the liver. Therefore, the quantitation was for a total amount of pyrrole−protein adducts generated and is presented as the molarity of a total pyrrole moiety released from all adducts present in the volume of blood (nM) or amount of liver (pmol/g) samples, respectively.

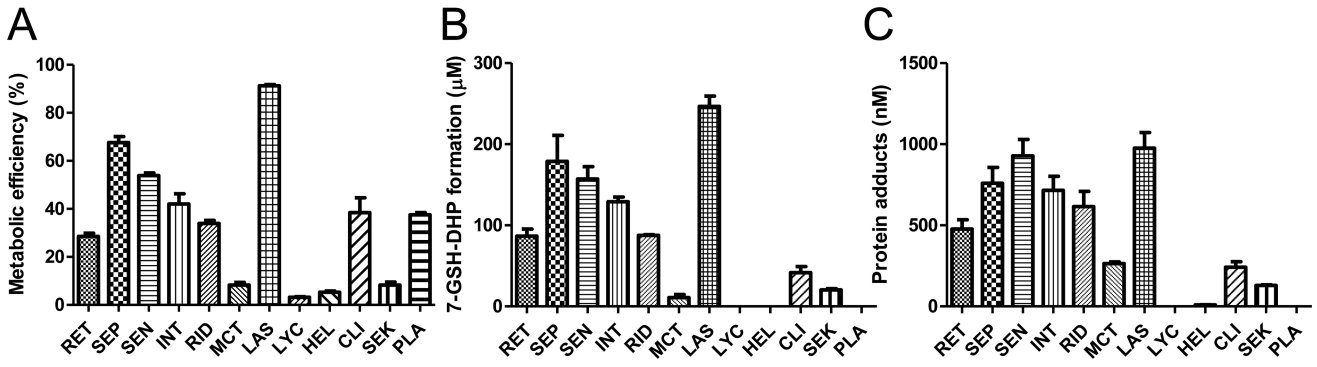

Figure 5. Metabolic efficiency (A), 7-GSH-DHP formation (B), and pyrrole−protein adduct formation (C) in the human liver microsomal incubations with different PAs.

HPLC-UV Analysis. Quantitative analysis of the parent PAs and pyrrole−GSH conjugates was completed on an Agilent series 1100 HPLC system (Agilent Technologies, Santa Clara, CA, USA) equipped with a vacuum degasser, a binary pump, an autosampler and a diode array detector. Sample separation was achieved on a Waters Symmetry C_{18} column (150 mm × 4.6 mm, 5 μm). The column temperature was maintained at 25 °C, and the flow rate was at 1.0 mL/min. Injection volume was 50 μL. Both parent PAs and pyrrole−GSH conjugates were monitored at 230 nm, and their UV absorption spectra were recorded over 200−400 nm. The mobile phases consisted of water containing 10 mM ammonium acetate (adjust pH to 5 with acetic acid) and acetonitrile, and a gradient elution was adopted as 2%−40% acetonitrile during 0−60 min. The intact PAs and 7,9-diGSH-DHP in the human liver microsomal incubated samples (n = 3) were quantified via constructing calibration curves using the corresponding standards. The metabolic efficiency of individual PAs were calculated as metabolic efficiency (%) = $(C_0 - C_{2h}/C_0) \times 100\%$. Where, C_0 is the concentration of the intact PA in the incubation mixture prior to incubation, and C_{2h} is the concentration of the intact PA in the incubation mixture after incubation for 2 h.

UHPLC-MS Analysis. UPLC-MS analysis was performed on an Agilent 6430 Triple Quadrupole LC/MS System using a Waters Acquity BEH C_{18} column (2.1 × 100 mm, 1.7 mm). The mobile phase of water containing 0.1% formic acid and acetonitrile was used with a gradient elution program as follows: 0−5 min, 35−95% acetonitrile; 5−5.5 min, 95% acetonitrile; and 5.5−6 min, 95−35% acetonitrile. The flow rate was 0.3 mL/min. The injection volume was 2 μL. The mass spectrometer was operated in multiple reaction monitoring (MRM) (transition m/z 341.2 > 252.2) in positive ion mode with an electrospray ionization interface and mass range of m/z 100−600. The fragmentor and collision energy were set at 185 and 33 V, respectively.

RESULTS

Protein Adducts Formed *in Vivo*. A total of 12 PAs (nine retronecine-type, two otonecine-type, and one platynecine-type) were studied. The retronecine-type PAs were further classified into four subgroups: including five 12-membered macrocyclic diesters (retrorsine, riddelliine, senecionine, seneciphylline and integerrimine); one 11-membered macrocyclic diester (monocrotaline); one open-ring diester (lasiocarpine); and two monoesters (heliotrine and lycopsamine) (Figure 1B). Pyrrole−protein adducts were examined in the blood and liver samples collected from the mice treated with different PAs. The UHPLC-MS MRM chromatograms of blood levels of pyrrole−protein adducts in mice treated with integerrimine, senkirkine, and platyphylline, representing the three types of PAs, respectively, are shown in Figure 3A. Pyrrole−protein adducts were detected in blood (Figure 3A,B) and liver specimens (Figure 3C) obtained from the mice treated with all retronecine-type and otonecine-type PAs but not in the mice treated with vehicle control or platyphylliine, a non/less-toxic platynecine-type PA. The results demonstrated that only PAs having an unsaturated necine base undergo metabolic activation to generate pyrrole−protein adducts associated with toxicity.

For nine retronecine-type PAs tested, except for lasiocarpine, which produced the highest pyrrole−protein adducts level in the blood and the second/third highest adduct level in the liver, the tendencies of pyrrole−protein adducts formed by different PAs in the liver was similar to that in the blood (Figure 3B,C) with the order of integerrimine > senecionine > retrorsine ≈ riddelliine > seneciphylline ≫ monocrotaline ≫ lycopsamine ≥ heliotrine. In both liver and blood, pyrrole−protein adduct levels generated by the 12-membered macrocyclic diester subgroup (integerrimine, retrorsine, seneciphylline, senecionine, and riddelliine) and the open-ring diester subgroup (lasiocarpine) of PAs were higher than that formed from the 11-membered macrocyclic diester PA (monocrotaline). Negligible amounts of pyrrole−protein adducts (about 1 pmol/g (liver) or nM (blood)) were detected in the mice treated with the two monoester PAs tested (lycopsamine and heliotrine). In the case of two otonecine-type 12-membered macrocyclic diester PAs (clivorine and senkirkine) tested, both liver and blood pyrrole−protein adduct levels were significantly lower than those generated by all retronecine-type 12-membered macrocyclic diester PAs. Although similar blood levels of pyrrole−protein adducts were generated by these two PAs, compared with clivorine, senkirkine formed much more adducts in the liver of the treated mice. The results demonstrated significant differences in metabolic activation efficiencies of PAs due to their structural differences, which are warranted for further investigation of their structure−toxicity relationship.

Metabolism of Different PAs by Human Liver Microsomes. Therefore, further systematic investigation of differences in metabolic activation efficiencies of different PAs was performed in the *in vitro* study. HPLC-UV chromatograms of the incubates obtained from human liver microsomal incubations with PAs, which are representative of the three different types, are shown in Figure 4. The metabolic profiles differed significantly among microsomal reactions with different types of PAs. As shown in Figure 4B,C, incubation of integerrimine and senkirkine, representatives of the retronecine-type and otonecine-types of toxic PAs, respectively, with human liver microsomes in the presence of GSH, generated the pyrrole−GSH conjugate 7-GSH-DHP. By contrast, no

dx.doi.org/10.1021/tx500071q | *Chem. Res. Toxicol.* 2014, 27, 1030−1039

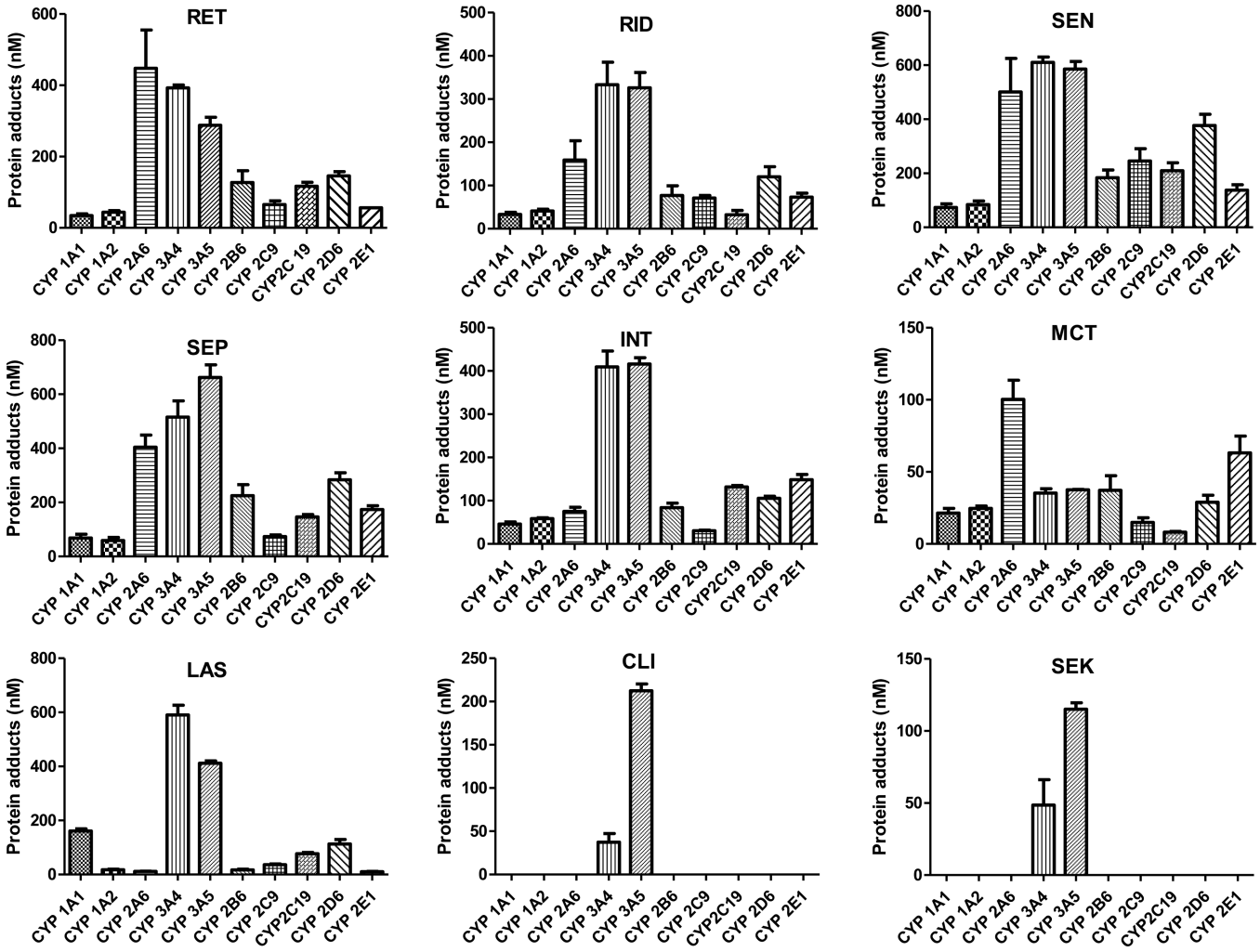

Figure 6. Pyrrole−protein adduct formation in the individual human recombinant CYP Supersome incubations with different PAs. Abbreviations used for individual PAs: retrorsine, RET; seneciphylline, SEP; senecionine, SEN; integerrimine, INT; riddelliine, RID; monocrotaline, MCT; lasiocarpine, LAS; clivorine, CLI; and senkirkine, SEK.

pyrrole−GSH conjugate was detected after incubation with platyphylline, a representative platynecine-type PA. Similarly, pyrrole−protein adducts were determined in the incubations of human liver microsomes with all retronecine-type and otonecine-type PAs but not in the incubation with platynecine-type platyphylline. These results further demonstrated that both of the toxic types of PAs having unsaturated necine bases but not the platyphylline type of PAs having a saturated necine base were metabolically activated to the reactive pyrrolic ester intermediates, which then interact with GSH to form pyrrole−GSH conjugates or with protein to generate pyrrole−protein adducts. However, the absence of both pyrrole−GSH conjugate and pyrrole−protein adducts when the platynecine-type PA platyphilline was incubated with human microsomes confirmed that no reactive pyrrolic intermediates were generated from this non/less-toxic PA. Moreover, it is noted that the failure to form pyrrolic adducts was observed, despite the fact that about 40% of the added platyphilline was metabolized with an amount comparable to those of several toxic PAs metabolized under the same microsomal reaction (Figure 5A). These results indicated that platyphilline has a different metabolic end point from that of the toxic PAs.

However, for all toxic PAs tested, the amounts of pyrrole−GSH conjugate formed were significantly higher than that of the pyrrole−protein adducts formed, but the tendency of 7-GSH-DHP formation (Figure 5B) by different PAs was similar to that of pyrrole−protein adduct formation (Figure 5C). Moreover, the tendency of pyrrole−protein adduct formation of all retronecine-type PAs determined in the liver and blood obtained from the treated mice was very similar to that observed in the *in vitro* incubation using human liver microsomes. In the case of otonecine-type PAs, the pattern of pyrrole−protein adducts levels detected in the human liver microsomal reactions correlated better with the pattern of pyrrole−protein adducts observed in the liver of the treated mice.

Human CYPs Mediating the Metabolic Activation of Different PAs. Human recombinant CYP Supersomes were incubated with different PAs to further investigate the CYPs catalyzing the metabolic activation of PAs by monitoring pyrrole−protein adducts. On the basis of the aforementioned results obtained from both *in vivo* and *in vitro* studies, no or negligible amounts of pyrrole−protein adducts were detected in experiments using platyphylline (non/less-toxic platynecine-type PA), lycopsamine, and heliotrine (monoesters of retronecine-type PA). Thus, these three PAs were not included

dx.doi.org/10.1021/tx500071q | *Chem. Res. Toxicol.* 2014, 27, 1030−1039

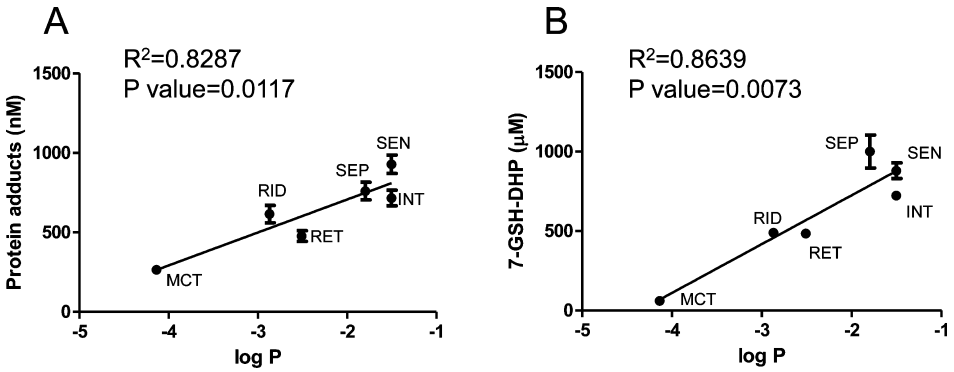

Figure 7. Correlation between the log *P* value and pyrrole−protein adduct formation in the human liver microsomal incubations with different macrocyclic diester PAs (A), and the correlation between the log *P* value and the 7-GSH-DHP conjugate formation in the human liver microsomal incubations with different macrocyclic diester PAs (B) tested using Pearson's correlation analysis. Abbreviations used for individual PAs: retrorsine, RET; seneciphylline, SEP; senecionine, SEN; integerrimine, INT; riddelliine, RID; and monocrotaline, MCT.

in the following human CYPs test. The remaining nine PAs were incubated with recombinant human CYP isoforms individually, and the results are shown in Figure 6. For retronecine-type PAs, CYP3A4 and CYP3A5 showed the highest activities for all PAs except for monocrotaline. Among the five retrornecine-type 12-membered macrocyclic diesters, CYP2A6 exhibited similar activities for retrorsine and senecionine, much lower activities for riddelliine and seneciphylline, but significantly less activity for integerrimine. For catalyzing the other two retrornecine-type PAs, CYP3A4 and CYP3A5 predominantly mediated the formation of pyrrole−protein adducts of lasiocarpine, an open-ring diester, while CYP2A6 exhibited the greatest activity in mediating the 11-membered macrocyclic diester monocrotaline. Moreover, a total of 10 CYPs, including the three mentioned above plus CYP1A1, CYP1A2, CYP2B6, CYP2C9, CYP2C19, CYP2D6, and CYP2E1, were all involved in mediating the metabolic activation of all 7 retronecine-type PAs investigated, although the catalytic activities of the later 7 CYPs were remarkably less. However, for mediating metabolic activation of the two otonecine-type PAs tested (clivorine and senkirkine), only CYP3A4 and CYP3A5 were proved to be involved with a remarkably higher activity of CYP3A5. While all other seven CYPs did not show any activity in catalyzing the formation of pyrrole−protein adducts.

DISCUSSION

Numerous toxic PAs with different structures occur in nature resulting in a high risk of PA exposure. However, their toxic potencies vary significantly.[6,10,12,32,33] Previously, Mattocks investigated the structure−toxicity relationship of various retronecine-type PAs and proposed that differences in toxicity might be mainly related to the structural features of their necine acids.[33] However, the structure−toxicity relationship among all three types of PAs has not been thoroughly investigated, and the detailed information in this regard is largely unknown. In the present study, we systematically investigated 12 different PAs representing three types and specifically assessed pyrrole−protein adducts to address the effects of different structures on PA metabolism-induced intoxication. In addition, the role of different CYP isoforms in mediating the metabolic activation of different PAs was also elucidated.

In the present study, first, both the *in vivo* and *in vitro* studies showed that among three different types of PAs platynecine-type PA did not produce pyrrole−protein adducts, which further confirmed that platynecine-type PAs are non/less-toxic due to the lack of metabolic activation as reported by Mattocks[26] and our previous studies.[7,34] By contrast, both retronecine-type and otonecine-type PAs underwent hepatic metabolic activation leading to pyrrole−protein adduct formation. Similarly, pyrrole−GSH conjugates were produced by both retronecine-type and otonecine-type PAs but not platynecine-type PAs *in vitro* and *in vivo*. GSH conjugation with reactive pyrrolic esters is generally recognized as the primary detoxification pathway for PAs.[3,26] In the present study, we found that the formation of pyrrole−GSH conjugates and pyrrole−protein adducts occurred simultaneously and competitively, as demonstrated by comparable formation rates of the conjugates generated by different PAs (Figure 5B,C). These results suggested that once the pyrrolic ester formed from metabolic activation, its intervention with protein is inevitable even in the presence of adequate amounts of GSH. Therefore, it is likely that even chronic exposure to low dosages of toxic PAs may lead to the accumulation of pyrrole−protein adducts and ultimately result in liver damage. Our results demonstrated that pyrrole−protein adducts can be utilized to evaluate the efficiency of metabolic activation and thus predict the toxic potencies of different PAs. Our findings also revealed that the unsaturated necine bases found in both retronecine-type and otonecine-type PAs were the most important structural determinant affecting the efficiency of hepatic metabolic activation, the formation rate of pyrrole−protein adducts in the liver, and the hepatotoxic potency.

Second, the formation rates of pyrrole−protein adducts determined in both *in vivo* and *in vitro* correlated well for the majority of toxic PAs tested, which provides a solid basis for using the level of pyrrole−protein adducts in the blood as a minimally invasive biomarker for clinical assessment and laboratory animal studies. In addition, our study demonstrated that the formation of pyrrole−protein adducts in the *in vitro* metabolic reactions performed with hepatic enzymes can be utilized for the mechanism-based structure−toxicity relationship investigation. On the basis of this rationale, we compared pyrrole−protein adduct levels in microsomal incubations with the two toxic types of 12-membered macrocyclic diester PAs. Our findings revealed that pyrrole−protein adducts formed by otonecine-type PAs were significantly lower than those by retronecine-type PAs having similar necine acids (Figure 1B). Because otonecine-type PAs require an additional oxidative *N*-demethylation step to form a pyrrolic ring structure prior to

dx.doi.org/10.1021/tx500071q | *Chem. Res. Toxicol.* 2014, 27, 1030−1039

generating the reactive pyrrolic ester[15] (Figure 2), this additional biotransformation step necessary to produce the reactive intermediate might reduce the overall rate of metabolic activation and the formation of pyrrole−protein adducts from otonecine-type of PAs.

Furthermore, among the nine retronecine-type PAs tested, the open-ring diester showed the highest efficiency for pyrrole−protein adduct formation, followed by the 12-membered macrocyclic diester and then by the 11-membered macrocyclic diester, while the monoester showed the lowest efficiencies. These differences can be attributed to structural differences in their necine acid groups because they all share the same necine base structure (Figure 1B). For the two monoester PAs, which possess a C7-hydroxyl group compared to the diester PAs with a C7-ester group, the significantly reduced metabolic activation and pyrrole−protein adduct formation were observed. Although, only PAs with C7-hydroxyl, but not C9-hydroxyl monoesters, were included in the study, our results are in a good agreement with those previously reported by Mattocks.[26] For the diesters, the metabolic activation rate of the open-ring diester (lasiocarpine) was much higher than that of macrocyclic diesters due to the reduced steric hindrance.[26] Moreover, lipophilicity also affected metabolic activation among PA macrocyclic diesters. The log *P* values (calculated by Advanced Chemistry Development (ACD/Laboratories) Software V11.02) of PAs correlated with the metabolic activation efficiency of retronecine-type macrocyclic diester PAs using Pearson's correlation analysis (Figure 7). For instance, PAs having log *P* values around −1.5 (log *P*: −1.504 (integerrimine), −1.796 (seneciphylline), and −1.504 (senecionine)) showed high efficiency, PAs with log *P* values of −2.5 to −2.9 (log *P*: −2.871 (riddelliine) and −2.509 (retrorsine)) had medium efficiency, while, monocrotaline with log *P* of −4.137 exhibited the lowest efficiency. These results agreed well with the observations of Mattocks[26] in that high lipophilicity makes PAs more susceptible to metabolic activation, while hydrophilic PAs tend to be excreted more readily, generate relatively low levels of reactive metabolites, and exhibit less hepatotoxic potency.

Finally, human hepatic enzymes mediating the metabolic activation of different PAs were thoroughly investigated. Previous studies focused mainly on species and gender differences in the enzymes catalyzing the metabolic activation of PAs, and CYP3A and CYP2B subfamilies were reported as the major enzymes mediating the metabolic activation of PAs in both animals and humans.[3,16,26,35−37] Our findings delineated different enzymatic profiles catalyzing the metabolic activation between the two types of toxic PAs. For otonecine-type PAs, only CYP3A4 and CYP3A5 predominantly mediated metabolic activation, while the 10 CYPS tested, including CYP1A1, CYP1A2, CYP2A6, CYP3A4, CYP3A5, CYP2B6, CYP2C9, CYP2C19. CYP2D6, and CYP2E1, all exhibited variable abilities to catalyze the metabolic activation of retronecine-type PAs. These enzymatic differences in mediating the metabolic activation of two different toxic types of PAs are mainly due to the specific enzymatic reaction for additional oxidative *N*-demethylation of otonecine-type PAs. It is also worthwhile to note that for retronecine-type of PAs, CYP3A4 and CYP3A5 exhibited the most prominent efficiencies for forming pyrrole−protein adducts from the open-ringed diester lasiocarpine. CYP3A4 and CYP3A5 also exhibited significantly high activities for all 12-membered macrocyclic diesters, while CYP2A6 also exhibited a very high activity for this group of PAs. However, for the 11-membered macrocyclic diester monocrotaline, CYP2A6 rather than CYP3A4 and CYP3A5 predominantly catalyzed the metabolic activation. By comparison with PAs activated predominantly by CYP3A4, the relatively low hepatotoxic potency associated with monocrotaline might be due to the relatively lower expression and activity of CYP2A6 in the liver, in contrast to the much higher activity of CYP3A4, which plays a dominant role in metabolizing a majority of drugs in the liver.[38,39]

In conclusion, the unsaturated necine base susceptible to hepatic metabolic activation is the core structure for PA intoxication, and retronecine-type PAs are much more susceptible than that of otonecine-type PAs. Among the same type of PAs, variations in the number of ester substitutions, lipophilicity, and steric hindrance of the necine acid groups could significantly affect the rate of metabolic activation. Furthermore, our results proved that, for the first time, the panel of CYPs capable of mediating metabolic activation of retronecine-type PAs is remarkably more diverse than that for otonecine-type PAs (10 CYPs vs 2 CYPs), which might contribute to the differences in hepatotoxic potency between these two types of toxic PAs. Our findings also provided scientific evidence for differences in PA intoxication from structural and enzymatic bases and established a structure-based rationale for the potential prediction of the hepatotoxicity of individual PAs.

AUTHOR INFORMATION

Corresponding Author

*Tel: +852 39436824. Fax: +852 26035139. E-mail: linge@cuhk.edu.hk.

Funding

The present study was supported by Research Grant Council of Hong Kong for GRF Grants (ref. no. 471013 and 469712) and The Chinese University of Hong Kong for the Direct Grant (ref. no. 4054047).

Notes

This article is not an official U.S. Food and Drug Administration (FDA) guidance or policy statement. No official support or endorsement by the U.S. FDA is intended or should be inferred.

The authors declare no competing financial interest.

ACKNOWLEDGMENTS

We thank Dr. Po-Chuen Chan for the gift of riddelliine and Professor Hai Shen Chen for the gift of integerrimine and platyphylline.

ABBREVIATIONS

PA, pyrrolizidine alkaloid; CYP, cytochrome P450; GSH, glutathione; MRM, multiple reaction monitoring; UHPLC-MS, ultrahigh pressure liquid chromatography−mass spectrometry

REFERENCES

(1) Chung, W. G., and Buhler, D. R. (1994) The effect of spironolactone treatment on the cytochrome P450-mediated metabolism of the pyrrolizidine alkaloid senecionine by hepatic microsomes from rats and guinea pigs. *Toxicol. Appl. Pharmacol. 127*, 314−319.

(2) Li, N., Xia, Q., Ruan, J., Fu, P. P., and Lin, G. (2011) Hepatotoxicity and tumorigenicity induced by metabolic activation of pyrrolizidine alkaloids in herbs. *Curr. Drug Metab. 12*, 823−834.

(3) Fu, P. P., Xia, Q., Lin, G., and Chou, M. W. (2004) Pyrrolizidine alkaloids–genotoxicity, metabolism enzymes, metabolic activation, and mechanisms. *Drug Metab. Rev. 36*, 1−55.
(4) Kakar, F., Akbarian, Z., Leslie, T., Mustafa, M. L., Watson, J., van Egmond, H. P., Omar, M. F., and Mofleh, J. (2010) An outbreak of hepatic veno-occlusive disease in Western afghanistan associated with exposure to wheat flour contaminated with pyrrolizidine alkaloids. *J. Toxicol. 2010*, 313280.
(5) Schneider, J., Tsegaye, Y., Tensae, M., Selassie, S. M., Haile, T., Bane, A., Ali, A., Mesfin, G., and Seboxa, T. (2012) Veno-occlusive liver disease: a case report. *Ethiop. Med. J. 50* (Suppl 2), 47−51.
(6) Mattocks, A. R. (1968) Toxicity of pyrrolizidine alkaloids. *Nature 217*, 723−728.
(7) Ruan, J., Liao, C., Ye, Y., and Lin, G. (2014) Lack of metabolic activation and predominant formation of an excreted metabolite of nontoxic platynecine-type pyrrolizidine alkaloids. *Chem. Res. Toxicol. 27*, 7−16.
(8) Ma, B., Li, N., and Lin, G. (2012) Importance of metabolic activation study to the safe use of Chinese herbal medicines. *Curr. Drug Metab. 13*, 652−658.
(9) Rieben, W. K., Jr., and Coulombe, R. A. (2004) DNA cross-linking by dehydromonocrotaline lacks apparent base sequence preference. *Toxicol. Sci. 82*, 497−503.
(10) Kim, H. Y., Stermitz, F. R., and Coulombe, R. A. (1995) Pyrrolizidine alkaloid-induced DNA-protein cross-links. *Carcinogenesis 16*, 2691−2697.
(11) Coulombe, R. A., Drew, G. L., and Stermitz, F. R. (1999) Pyrrolizidine alkaloids crosslink DNA with actin. *Toxicol. Appl. Pharmacol. 154*, 198−202.
(12) Kim, H. Y., Stermitz, F. R., Molyneux, R. J., Wilson, D. W., Taylor, D., and Coulombe, R. A. (1993) Structural influences on pyrrolizidine alkaloid-induced cytopathology. *Toxicol. Appl. Pharmacol. 122*, 61−69.
(13) Kim, H. Y., Stermitz, F. R., Li, J. K., and Coulombe, R. A. (1999) Comparative DNA cross-linking by activated pyrrolizidine alkaloids. *Food Chem. Toxicol. 37*, 619−625.
(14) Hincks, J. R., Kim, H. Y., Segall, H. J., Molyneux, R. J., Stermitz, F. R., and Coulombe, R. A. (1991) DNA cross-linking in mammalian cells by pyrrolizidine alkaloids: structure−activity relationships. *Toxicol. Appl. Pharmacol. 111*, 90−98.
(15) Lin, G., Cui, Y. Y., and Hawes, E. M. (2000) Characterization of rat liver microsomal metabolites of clivorine, an hepatotoxic otonecine-type pyrrolizidine alkaloid. *Drug Metab. Dispos. 28*, 1475−1483.
(16) Chung, W. G., and Buhler, D. R. (2004) Differential metabolism of the pyrrolizidine alkaloid, senecionine, in Fischer 344 and Sprague-Dawley rats. *Arch. Pharm. Res. 27*, 547−553.
(17) Lin, G., Cui, Y. Y., and Hawes, E. M. (1998) Microsomal formation of a pyrrolic alcohol glutathione conjugate of clivorine. Firm evidence for the formation of a pyrrolic metabolite of an otonecine-type pyrrolizidine alkaloid. *Drug Metab. Dispos. 26*, 181−184.
(18) Kasahara, Y., Kiyatake, K., Tatsumi, K., Sugito, K., Kakusaka, I., Yamagata, S., Ohmori, S., Kitada, M., and Kuriyama, T. (1997) Bioactivation of monocrotaline by P-450 3A in rat liver. *J. Cardiovasc. Pharmacol. 30*, 124−129.
(19) Miranda, C. L., Reed, R. L., Guengerich, F. P., and Buhler, D. R. (1991) Role of cytochrome P450IIIA4 in the metabolism of the pyrrolizidine alkaloid senecionine in human liver. *Carcinogenesis 12*, 515−519.
(20) Lin, G., Wang, J. Y., Li, N., Li, M., Gao, H., Ji, Y., Zhang, F., Wang, H., Zhou, Y., Ye, Y., Xu, H. X., and Zheng, J. (2011) Hepatic sinusoidal obstruction syndrome associated with consumption of *Gynura segetum*. *J. Hepatol. 54*, 666−673.
(21) Gao, H., Li, N., Wang, J. Y., Zhang, S. C., and Lin, G. (2012) Definitive diagnosis of hepatic sinusoidal obstruction syndrome induced by pyrrolizidine alkaloids. *J. Dig. Dis. 13*, 33−39.
(22) U.S. Food and Drug Administration (2001) FDA Advises Dietary Supplement Manufacturers to Remove Comfrey Products from the Market, available at http://www.fda.gov/Food/RecallsOutbreaksEmergencies/SafetyAlertsAdvisories/ucm111219.htm (accessed Jul 6, 2001).
(23) U.K. Medicines and Healthcare Products Regulatory Agency (2007) Proposals to Prohibit the Sale, Supply or Importation of Unlicensed Medicinal Products for Internal Use Which Contain Senecio Species and Proposals to Amend Three Existing Orders, available at http://www.mhra.gov.uk/Publications/Consultations/Medicinesconsultations/Othermedicinesconsultations/CON2030747 (accessed Mar 27, 2007).
(24) Bundesgesundheitsamt (German Federal Health Bureau) (1992) Bekanntmachung über die Zulassung und Registrierung von Arzneimitteln (Abwehr von Arzneimittelrisiken − Stufe II). *Bundesanzeiger 111*, 4805−4807.
(25) International Program on Chemical Safety (1989) *Health and Safety Guide No. 26: Pyrrolizidine Alkaloids Health and Safety Guide*, World Health Organization, Geneva, Switzerland.
(26) Mattocks, A. R. (1968) Chemistry and Toxicology of Pyrrolizidine Alkaloids, *Relationships between Structure, Metabolism and Toxicity*, pp 320−325, Academic Press, London.
(27) Lin, G., Zhou, K. Y., Zhao, X. G., Wang, Z. T., and But, P. P. (1998) Determination of hepatotoxic pyrrolizidine alkaloids by on-line high performance liquid chromatography-mass spectrometry with an electrospray interface. *Rapid Commun. Mass Spectrom. 12*, 1445−1456.
(28) Lin, G., Rose, P., Chatson, K. B., Hawes, E. M., Zhao, X. G., and Wang, Z. T. (2000) Characterization of two structural forms of otonecine-type pyrrolizidine alkaloids from *Ligularia hodgsonii* by NMR spectroscopy. *J. Nat. Prod. 63*, 857−860.
(29) Chan, P. C., Haseman, J. K., Prejean, J. D., and Nyska, A. (2003) Toxicity and carcinogenicity of riddelliine in rats and mice. *Toxicol. Lett. 144*, 295−311.
(30) Lin, G., Nnane, I. P., and Cheng, T. Y. (1999) The effects of pretreatment with glycyrrhizin and glycyrrhetinic acid on the retrorsine-induced hepatotoxicity in rats. *Toxicon 37*, 1259−1270.
(31) Lin, G., Tang, J., Liu, X. Q., Jiang, Y., and Zheng, J. (2007) Deacetylclivorine: a gender-selective metabolite of clivorine formed in female SD rat liver microsomes. *Drug Metab. Dispos. 35*, 607−613.
(32) Li, Y. H., Kan, W. L., Li, N., and Lin, G. (2013) Assessment of pyrrolizidine alkaloid-induced toxicity in an *in vitro* screening model. *J. Ethnopharmacol. 150*, 560−567.
(33) Mattocks, A. R. (1981) Relation of structural features to pyrrolic metabolites in livers of rats given pyrrolizidine alkaloids and derivatives. *Chem.-Biol. Interact. 35*, 301−310.
(34) Xia, Q., Zhao, Y., Von Tungeln, L. S., Doerge, D. R., Lin, G., Cai, L., and Fu, P. P. (2013) Pyrrolizidine alkaloid-derived DNA adducts as a common biological biomarker of pyrrolizidine alkaloid-induced tumorigenicity. *Chem. Res. Toxicol. 26*, 1384−1396.
(35) Lin, G., Cui, Y. Y., and Liu, X. Q. (2003) Gender differences in microsomal metabolic activation of hepatotoxic clivorine in rat. *Chem. Res. Toxicol. 16*, 768−774.
(36) Xia, Q., Chou, M. W., Kadlubar, F. F., Chan, P. C., and Fu, P. P. (2003) Human liver microsomal metabolism and DNA adduct formation of the tumorigenic pyrrolizidine alkaloid, riddelliine. *Chem. Res. Toxicol. 16*, 66−73.
(37) Xia, Q., Chou, M. W., Lin, G., and Fu, P. P. (2004) Metabolic formation of DHP-derived DNA adducts from a representative otonecine type pyrrolizidine alkaloid clivorine and the extract of *Ligularia hodgsonnii* hook. *Chem. Res. Toxicol. 17*, 702−708.
(38) Klein, K., and Zanger, U. M. (2013) Pharmacogenomics of cytochrome P450 3A4: recent progress toward the "missing heritability" problem. *Front. Genet. 4*, 12, DOI: 10.3389/fgene.2013.00012.
(39) Lamba, J. K., Lin, Y. S., Schuetz, E. G., and Thummel, K. E. (2002) Genetic contribution to variable human CYP3A-mediated metabolism. *Adv. Drug Delivery Rev. 54*, 1271−1294.